RSC Advances

PAPER

View Article Online
View Journal | View Issue

Cite this: *RSC Adv.*, 2024, **14**, 29860

Influences of topography on nitrate export from forested watersheds on Yakushima Island, a Natural World Heritage site†

Ken'ichi Shinozuka, *[a] Osamu Nagafuchi, [b] Koyomi Nakazawa, [c] Urumu Tsunogai, [d] Fumiko Nakagawa,[d] Kenshi Tetsuka,[e] Natsumi Tetsuka[e] and Senichi Ebise[f]

In East Asia, high levels of atmospheric nitrogen are deposited onto land. This could elevate the nitrate levels in coastal waters *via* river runoff, even from areas where anthropogenic sources are minimal. It is important to identify NO_3^- sources in river water and the mechanisms involved in NO_3^- runoff. Yakushima Island, Japan, is a Natural World Heritage site featuring numerous watersheds with diverse topography and rivers. The area receives significant precipitation, with up to 10 000 mm in mountainous regions. Its proximity to coastal urban areas in China (~800 km) leads to substantial atmospheric nitrogen wet and dry deposition in the island's forests. The study aimed to clarify regional water quality characteristics by conducting long-term monitoring of dissolved ion components (Na^+, K^+, Mg^{2+}, Ca^{2+}, F^-, Cl^-, NO_3^-, and SO_4^{2-}) in river waters, and to determine the effects of NO_3^- sources and watershed topography on NO_3^- behavior. Dissolved ion concentrations were obtained from a long-term monitoring (2011–2014) dataset. Cluster analysis classified runoff water from the central mountainous region into three groups: western region, other regions, and groundwater. The average NO_3^- concentration in the western region was 10.2 μmol L^{-1}, which was higher than the 6.24 μmol L^{-1} observed in the other regions. Stable isotope analysis in December 2018 showed that river water NO_3^- (1.39 μmol L^{-1}) in the western region had a high proportion of atmospheric NO_3^-. Topographic analysis indicated that NO_3^- and atmospheric NO_3^- increased in smaller watersheds and steeper terrain. This study conclude that NO_3^- output is controlled by topography.

Received 7th June 2024
Accepted 3rd September 2024

DOI: 10.1039/d4ra04168b

rsc.li/rsc-advances

1 Introduction

Yakushima Island has a rich natural forest and is a Natural World Heritage site, but there have long been concerns about acidification of the rivers on the island. The island experiences acid wet deposition levels of 43.2 and 35.4 mmol m^{-2} per year (nss-SO_4^{2-} and NO_3^-, respectively), which are significantly higher than those recorded in major cities in Japan (*e.g.*, Tokyo: 17.1 and 25.6 mmol m^{-2} per year).[1] Soils and rivers on the island continue to be affected by groundwater and stream water acidification,[2,3] decreasing acid buffering capacities of soils in watersheds,[4,5] and the effects of long-term acid deposition from the atmosphere.[6] Precipitation on Yakushima Island contains large amounts of sea salt and anthropogenic S- and N-containing compounds.[7] The principal cause of acidification is air pollution from continental China, located northwest of the island across the East China Sea.[8–10] The transport pathways of pollutants in air mean that the northwest of the island is more affected by air pollution than the southeast.[3,11]

In unmanaged forest, atmospheric nitrogen deposition accounts for the majority of nitrogen input to the forest nitrogen cycle. Mountain forest ecosystems on islands are more sensitive than inland mountain forest ecosystems to atmospheric deposition. Mountain ecosystems are limited by the supply of N for long periods,[12] thus they are particularly sensitive to atmospheric deposition of N.[13–15] More N is deposited at high elevations, such as in mountainous areas, than at low elevations.[16] Islands with limited ecosystem resources[17] are vulnerable to external factors such as N deposition.[18] Pristine natural environments tend to have low N inputs, and organisms use limited N.[19,20] N deposition from the atmosphere will, therefore, strongly affect pristine natural environments.[15,21,22]

[a]*River Basin Research Center, Gifu University, 1-1 Yanagido, Gifu City, Gifu 501-1112, Japan. E-mail: kennichi97@gmail.com*
[b]*Environmental Science Institute, Comprehensive Research Organizations of Fukuoka Institute of Technology, Wajiro Higashi, Higashi-ku, Fukuoka 811-0295, Japan*
[c]*Department of Environmental and Civil Engineering, Toyama Prefectural University, 5180, Kurokawa, Imizu, Toyama 930-0975, Japan*
[d]*Graduate School of Environmental Studies, Nagoya University, Furo-cho, Chikusa-ku, Nagoya 464-8601, Japan*
[e]*Yakushima Institute of Environmental Sciences, Isso, Yakushima-cho, Kumage, Kagoshima 891-4203, Japan*
[f]*Faculty of Science and Engineering, Setsunan University, Ikedanakamachi, Neyagawa City, Osaka 572-8508, Japan*

† Electronic supplementary information (ESI) available. See DOI: https://doi.org/10.1039/d4ra04168b

Anthropogenic emissions of reactive N have dramatically increased the amount of available nitrogen in global ecosystems. Nitrate (NO_3^-) is water-soluble and one of the most important nutrients for primary production in the aquatic environment. Excess NO_3^- in river water can cause eutrophication, which can lead to severe ecological and economic problems downstream, such as in lakes, estuaries, and oceans.[23–25] Nitrogen oxide concentrations in East Asia have increased rapidly, peaking in approximately 2010, and have since begun to decrease, but atmospheric nitrogen oxide concentrations remain high.[26] Nitrogen oxides affect the nitrogen cycle in leeward forests and oceans, regardless of national borders.[27,28]

In forests with high levels of nitrogen deposition, stream water NO_3^- is elevated, typically ranging between 100 and 200 μ mol L^{-1},[29,30] providing a nitrogen source for downstream ecosystems.[27,31] Interestingly, mountainous islands, even those without direct anthropogenic nitrogen sources, can exhibit high NO_3^- concentrations in river water due to atmospheric deposition.[32] Understanding the mechanisms behind nitrate runoff from forested areas that are free from direct human pollution will provide valuable insights for managing downstream nitrogen levels.

In previous studies, the sources of NO_3^- have been identified by analyzing nitrogen and oxygen stable isotope ratios ($\delta^{15}N$ and $\delta^{18}O$).[33,34] Determining $\delta^{17}O$ also allows a clear distinction to be made between NO_3^- deposited from the atmosphere ($NO_3^-{}_{atm}$) and NO_3^- produced through biological processes ($NO_3^-{}_{re}$).[35,36] $\Delta^{17}O$ analysis is a powerful tool for investigating the N cycle in forested areas, and has been used to indicate nitrogen saturation,[37] N cycling in the European Alps,[38] and N cycling in forests.[37–45] Furthermore, forested streams with high NO_3^- concentrations in the stream water have higher $\Delta^{17}O$ because atmospheric nitrate is not incorporated into the forest nitrogen cycle, but instead flows out.[37,46]

The aim of this study was to identify the sources of dissolved NO_3^- in rivers in forests on Yakushima Island, where most of the N input comes from atmospheric deposition or nitrification. There are many rivers in forested areas with various topographies, meaning that the residence times in different catchments are likely to be different. We identified which rivers were sensitive to atmospheric deposition of nitrogen. First, rivers were classified by region using the results of long-term sampling and analyses of dissolved ionic components. Next, the sources of NO_3^- in river water in the winter were identified and the influence of the topography of each catchment on the sources of NO_3^- in river water in the catchment was investigated. We hypothesized that because differences in vegetation are less likely to affect river water quality in winter, more NO_3^- of atmospheric origin will be deposited into the river water, which is clearly correlated with the topography (especially residence time).

2 Materials and methods

2.1 Site description

Yakushima Island (30.34°N, 130.51°E) is ~800 km east of Shanghai (China) and ~60 km south–southwest of Cape Sata in Kagoshima (Japan), and separates the East China Sea and the Pacific Ocean (Fig. 1). The island is circular and has an area of ~504 km^2, with 10 mountain ranges in the center (the Central Mountains Group) with elevations of 1800 m or more, including the highest peak in Kyushu, Mount Miyanoura (1935 m), and 46 mountain ranges[47] with elevations of ~1000 m around the island's edges. The island has subtropical to subarctic climate zones from coast to summit, which is unusual at the latitude of the island. Warm air (from warm oceanic currents) containing large amounts of water vapor rises over the mountains, resulting in large amounts of precipitation. Annual precipitation is ~4500 mm^{-1} on the plains and >10 000 mm^{-1} in the mountains.[48] This is one reason why Yakushima Island is also called "the Alpine mountains of the sea". Yakushima Island is very biodiverse and has a unique range of ecosystems adapted to the humid environment. There are many Yaku cedar (*Cryptomeria japonica*), which are rare elsewhere in the world and can live for thousands of years. These factors led to ~20% of Yakushima Island becoming a Natural World Heritage site in 1993.[49] The western part of the island has particularly rugged terrain and is a Natural World Heritage site from the coastline to the mountain peaks.[50] No people live in the western region and the landscape is forested. In other regions, habitable areas are concentrated in a few flat areas downstream near the coast. Therefore, by selecting the rivers and points to be surveyed, it was possible to eliminate the influence of anthropogenic pollution sources such as domestic wastewater. The sources of nitrogen input to the watershed could be investigated in watersheds where atmospheric nitrogen deposition and nitrogen fixation in the forest were the only sources of nitrogen input.

This western region has many streams, the headwaters of which are on Mount Kuniwari (1323 m above sea level), only 2 km from the coast. In regions other than the western region, rivers flow from the Central Mountain Range Group to and through the surrounding mountains. Groundwater emerge from many rocky crevices. Samples were collected from 22 sites on the main rivers, shown in Fig. 1. In this study, sampling was carried out on clear days. When it rains in the western region, the roads are closed in case of flooding, making it impossible to carry out surveys. In this area, bridges often wash away, making it unviable to travel around the island. It is dangerous and impossible to conduct surveys at times when it is raining and $NO_3^-{}_{atm}$ levels are likely to be high. When we were able to get close to a river, we filled a bottle with river water to collect samples. When we were unable to get close to a river, we used a bucket to collect a river water sample from a bridge. The bucket was lowered into the middle of the river where the water was thought to be well mixed. We grab sampled water from rivers around Yakushima Island over a day of travel. Water samples were collected, and field observations were made along the major rivers at points where no anthropogenic pollution occurred (Table 1). To select the sampling sites, we used GIS to calculate the land use area of the watershed and confirmed on-site that the land use area upstream was forest. The study period was January 2011 to March 2014. Twice monthly samples were collected from the main rivers on Yakushima Island. The

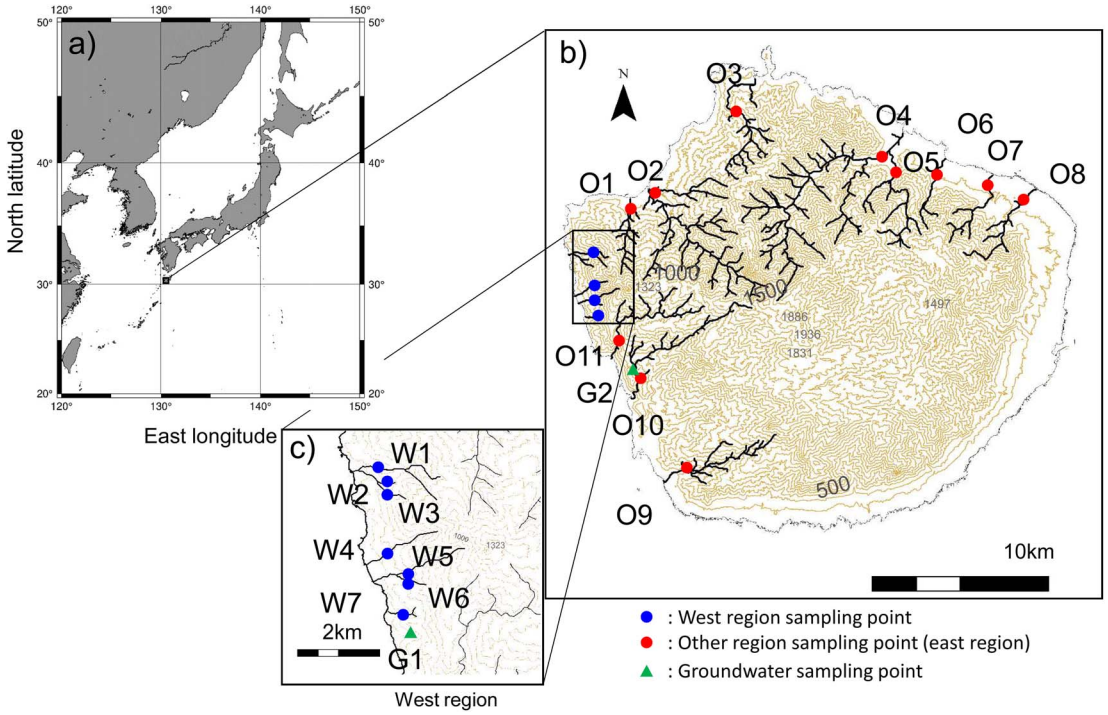

Fig. 1 Maps showing: (a) the location of Yakushima Island, (b) the main rivers in forested areas and groundwater sampling sites, and (c) the rivers in the western region of Yakushima Island from which samples were collected. Blue circles indicate rivers in the western region, red circles indicate rivers in other regions, and green triangles indicate groundwater.

surveys conducted during this period aimed to clarify the trends in ionic components of river water in Yakushima Island. An additional study was performed on 19 December 2018 to identify the sources of NO_3^- in river water during the winter. In this survey, stable isotope ratios were used to estimate the source of NO_3^- in river water.

2.2 Chemical analysis

After collection, each river or groundwater sample was transported to the laboratory and immediately passed through a 0.45 μm membrane disc filter (DISMIC-25CS; Advantec, Tokyo, Japan) and then stored at 4 °C in a dark place. Dissolved ions were determined using a Compact IC 761 ion chromatograph

Table 1 Land use ratio and topography indicators for the study area. TWI is the topographic wetness index. TWI was calculated using eqn (3). The mean TWI is the average TWI of each watershed

		Forest (%)	Agricultural land (%)	Urban (%)	Area (km^2)	Mean altitude (m)	Mean slope (°)	Mean TWI
Western region	W1	100.0	0.0	0.0	1.94	569	33.2	4.88
	W2	100.0	0.0	0.0	0.29	489	33.4	4.72
	W3	100.0	0.0	0.0	0.29	522	33.0	4.72
	W4	100.0	0.0	0.0	1.14	596	39.0	4.68
	W5	100.0	0.0	0.0	1.44	740	39.4	4.68
	W6	100.0	0.0	0.0	0.14	468	34.5	4.80
	W7	100.0	0.0	0.0	0.36	530	32.9	4.88
Other regions	O1	99.5	0.5	0.0	7.06	551	29.0	5.00
	O2	99.3	0.1	0.0	27.93	827	34.1	4.83
	O3	100.0	0.0	0.0	10.54	537	27.0	5.06
	O4	100.0	0.0	0.0	37.16	747	32.5	4.92
	O5	100.0	0.0	0.0	12.81	684	29.0	5.03
	O6	98.0	2.0	0.0	3.70	496	28.6	5.09
	O7	98.7	1.3	0.0	5.64	528	30.7	5.01
	O8	97.5	2.5	0.0	7.62	406	26.8	5.23
	O9	98.3	1.5	0.2	11.82	535	26.0	5.15
	O10	100.0	0.0	0.0	12.07	820	25.9	5.18
	O11	100.0	0.0	0.0	12.36	928	25.4	5.18

(Metrohm, Herisau, Switzerland). The main dissolved ions (Na^+, K^+, NH_4^+, Mg^{2+}, Ca^{2+}, Cl^-, NO_3^-, and SO_4^{2-}) were determined. The measurement errors were ±4.22 μmol L^{-1} for Na^+, ±3.90 μmol L^{-1} for K^+, ±2.61 μmol L^{-1} for Mg^{2+}, ±2.37 μmol L^{-1} for Ca^{2+}, ±6.89 μmol L^{-1} for Cl^-, ±2.31 μmol L^{-1} for NO_3^-, and ±3.14 μmol L^{-1} for SO_4^{2-}. The NH_4^+ concentrations in the samples were <2.00 μmol L^{-1}.

The $\Delta^{17}O$, $\delta^{18}O$, and $\delta^{15}N$ values for NO_3^- in the water samples collected in December 2018 were determined after converting the NO_3^- into N_2O using the cadmium reduction method.[51–53] Oxygen isotopes in NO_3^- were determined if the NO_3^- concentration in a sample was >0.8 μmol L^{-1}. The N_2O produced was introduced into a gold wire oven (Agilent 6890; Agilent Technologies, Santa Clara, CA, USA) held at 780 °C to pyrolyze N_2O to give N_2 and O_2. The O_2 produced was then analyzed to give the ^{16}O, ^{17}O, and ^{18}O isotope composition using a Finnigan MAT252 isotope ratio mass spectrometer (Thermo Fisher Scientific, Waltham, MA, USA).[54,55] The instrument was calibrated using international nitrate standards (USGS-34 and USGS-35).[45,52,56] The measurement errors for the samples were ±0.38‰ for $\delta^{15}N$, ±0.5‰ for $\delta^{18}O$, and ±0.2‰ for $\Delta^{17}O$.

2.3 Nitrate in the atmosphere calculations

$NO_3^-{}_{re}$ generated through nitrification is produced from decomposing organic matter and the fixation of the released nitrogen. Most of the $NO_3^-{}_{atm}$ produced in the atmosphere is generated through photochemical reactions between atmospheric NO and O_3. The $NO_3^-{}_{atm}$ formation process can be characterized from anomalies in ^{17}O enrichment.[36,57] NO_3^-, including $NO_3^-{}_{atm}$, is produced through an assimilation, decomposition, and nitrification cycle and is converted into $NO_3^-{}_{re}$. The $\Delta^{17}O$–NO_3^- value (the magnitude of the excess ^{17}O produced in the atmosphere) was calculated using eqn (1),[58] which was used to distinguish between $NO_3^-{}_{atm}$ ($\Delta^{17}O > 0‰$) and $NO_3^-{}_{re}$ ($\Delta^{17}O = 0‰$).[37]

$$\Delta^{17}O = ((1 + \delta^{17}O)/(1 + \delta^{18}O)\beta) - 1 \quad (1)$$

The value of β was 0.5279.[58] Eqn (2) was used to calculate the ratio between the contributions of atmospheric nitric acid and regenerative nitric acid to the NO_3^- concentrations in the river and stream water samples.

$$NO_3^-{}_{atm}/NO_3^-{}_{in\ river} = \Delta^{17}O_{in\ rain}/\Delta^{17}O_{in\ river} \quad (2)$$

This allowed $\Delta^{17}O$–NO_3^- for stream water to be calculated. The $\Delta^{17}O$–NO_3^- value for precipitation in the Northern Hemisphere is +26.6 ± 0.9 (std) ‰.[36,57] The $\Delta^{17}O$–NO_3^- values for NO_3^- in precipitation in December 2018 on Yakushima Island were +23.0‰ (16 December 2018) and +28.3‰ (19 December 2018), which supported the $\Delta^{17}O$ values of nitrate in precipitation reported in previous studies (Table 2). The $NO_3^-{}_{atm}$ concentration could be calculated from eqn (2), thus the $NO_3^-{}_{re}$ concentration could be calculated by subtracting the $NO_3^-{}_{atm}$ concentration from the NO_3^- in stream water concentration.

2.4 Topographic wetness index analysis

In rugged terrain, such as in mountainous areas, each catchment will have a complex topography with various gradients. Detailed analysis taking spatially heterogeneous landforms into consideration can shed light on complex bio-geoscientific processes that occur over large areas in such terrain.[59,60] The catchment area, mean catchment slope, and topographic wetness index (TWI) were used as indicators of water retention related to the catchment topography (Table 1). The TWI indicates ponding of surface runoff and local variations in the groundwater table in TOPMODEL, which is a widely used precipitation runoff model for the small watershed scale, such as for watersheds in forests.[61] Locations with the same TWI value respond hydrologically in the same way and are, therefore, hydrologically similar. The TWI is also used to investigate the N cycle through identifying hydrologically similar areas.[62–66] Using the TWI value, it is possible to quantify the similarity of residence times between sampling watersheds. The catchment area, slope, and topographic wetness index (TWI) for each study site were calculated using ArcGIS (version 10.4.1) using data from a digital elevation model[67] with a resolution of 20 m × 20 m. The TWI was calculated using eqn (3).[63,68]

$$TWI = \ln(\alpha/\tan\beta) \quad (3)$$

In eqn (3), α is the upstream watershed area per contour unit discharged from a given point and β is the slope at a given point. The digital elevation model data had a resolution of 20 m × 20 m. One value was calculated for each 20 m × 20 m square. The TWI for each sampling site was calculated by calculating the mean of several TWIs for 20 m × 20 m squares in the catchment.

2.5 Statistical processing

Statistical processing involved calculating *K*-means, Welch's *t* test and performing linear regression analyses using R (version 4.1) software. The *K*-means results were classified using cluster,[69] which is an open source library in R. The *K*-means were calculated by performing 500 iterations using the Hartigan–Wong algorithm.

3 Results and discussion

3.1 Characteristics of Yakushima Island river water determined by long-term monitoring

The Na^+, K^+, Mg^{2+}, Ca^{2+}, F^-, Cl^-, NO_3^-, and SO_4^{2-} concentrations found in the 4-year long-term samples of all river water and groundwater were 340 ± 148, 12.3 ± 6.81, 36.8 ± 23.5, 27.4

Table 2 NO_3^- concentrations and stable isotope ratios in precipitation during the survey period 16–19 December 2019

Sampling date	NO_3^- (μmol L^{-1})	$\delta^{15}N$ (‰)	$\delta^{18}O$ (‰)	$\Delta^{17}O$ (‰)
16 December 2018	11.3	−2.94	74.23	17.98
19 December 2018	15.83	−0.03	90.81	22.26

$\pm$ 19.7, 2.57 $\pm$ 2.79, 312 $\pm$ 151, 7.56 $\pm$ 7.21, and 49.3 $\pm$ 20.3 μmol L^{-1}, respectively (Fig. S1†). Yakushima Island is surrounded by the sea, thus the river water contains many components derived from sea salt.[6] These ionic components change significantly depending on the season. The dissolved ion analysis results were subjected to cluster analysis, which divided the major rivers and groundwater into three groups (Fig. 2). Component 1 contained the Na^+, K^+, Ca^{2+}, Mg^{2+}, F^-, Cl^-, NO_3^-, and SO_4^{2-} components, and as the component value increased, the concentration of each ionic component increased. Component 2 contained the F^- and NO_3^- components, and as the component value increased, the F^- concentration increased, but the NO_3^- decreased. Ground water tended to have a higher rock content owing to its longer residence time, and the sea salt content tended to be higher in the western region closer to the coast compared with other regions. The cluster analysis results are shown in Table 3. Group 1 contained "other regions" (n = 469), group 2 contained the western region (n = 575), and group 3 contained groundwater (n = 103). These groups together accounted for ~90% of the samples (Table 3). There were 0 samples in groundwater classified as group 1, and 1 sample in other regions classified as group 3. This demonstrated that the other regions and groundwater had different ionic compositions. The water quality of rivers on Yakushima Island was found to be more affected by differences between the survey sites than by seasonal changes. In the next section, we identify trends for the different ions in the three groups (other regions, the western region, and groundwater).

Table 3 Matrix of the K-means classification results shown in Fig. 2. The K-means were used to divide the ionic components of groundwater in the western and eastern regions of Yakushima Island into three classes, and the number of samples in each class is shown

	Group 1	Group 2	Group 3
Western region	28	469	13
Other regions	575	41	1
Groundwater	0	11	103

The concentrations of ions in the other regions, western region, and groundwater are shown in Table 4. The dissolved ion concentrations except the NO_3^- concentration decreased in the order groundwater, western region, and other regions. The NO_3^- concentration decreased in the order western region (10.2 $\pm$ 8.39 μmol L^{-1}), other regions (6.24 $\pm$ 5.74 μmol L^{-1}), and groundwater (3.31 $\pm$ 3.57 μmol L^{-1}) (Fig. 3 and S1†). The Na to Cl ratio was 1.20 for other regions, 1.04 for the western region, and 1.14 for groundwater, with the ratio for the western region being significantly lower than the ratios for the other groups (p < 0.001) (Fig. 3a). Yakushima Island is composed of uniform granite except in coastal areas, and differences between

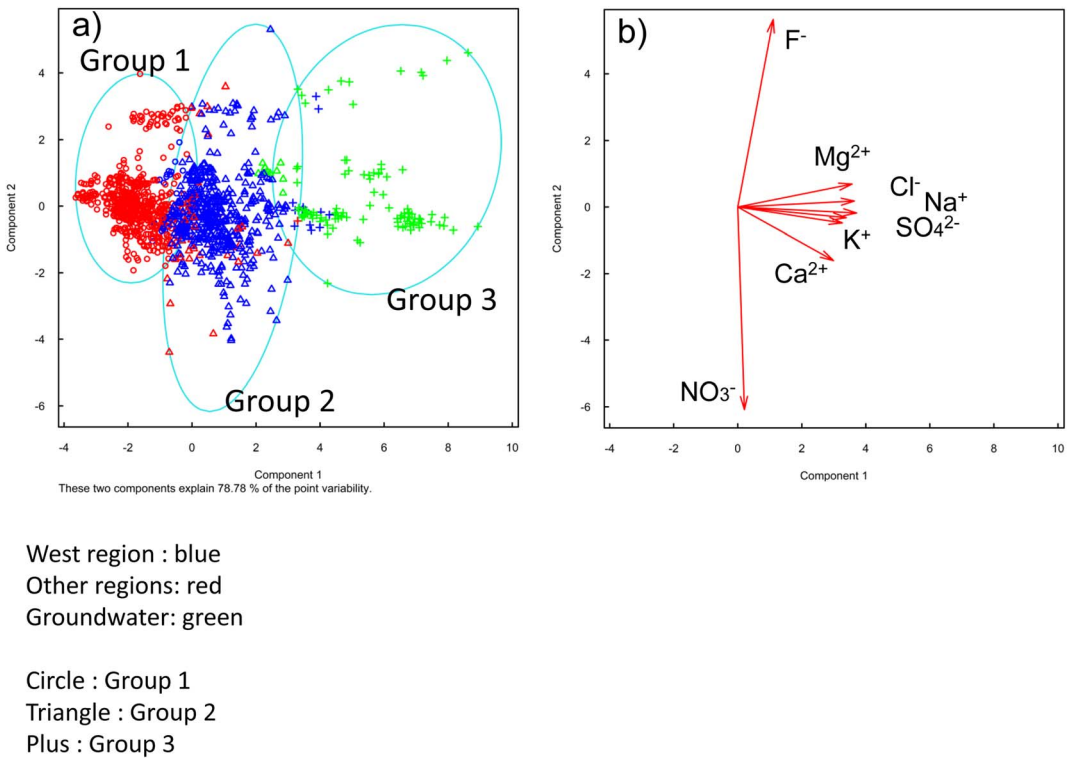

Fig. 2 Results of principal component analysis of the main ionic components determined in the long-term monitoring (2011–2014) study with two explanatory variables. (a) Sample components are shown in blue for the western region, red for the other regions, and green for groundwater. K-Means classification resulted in three classes (plus symbols: group 1, triangles: group 2, and circles: group 3). (b) The eight ion components Na^+, K^+, Ca^{2+}, Mg^{2+}, F^-, Cl^-, NO_3^-, and SO_4^{2-} are grouped into two components. Components 1 and 2 explained 79% of the ionic components.

Table 4 Major ionic component concentrations determined in the long-term monitoring study (2011–2014)

	Na^+ (μmol L^{-1})	K^+ (μmol L^{-1})	Mg^{2+} (μmol L^{-1})	Ca^{2+} (μmol L^{-1})	Cl^- (μmol L^{-1})	NO_3^- (μmol L^{-1})	SO_4^{2-} (μmol L^{-1})
Western region	392 ± 72.9	12.5 ± 3.03	41.6 ± 11.9	29.8 ± 13.3	380 ± 86.4	10.2 ± 8.39	62.1 ± 7.03
Other regions	236 ± 58.7	9.59 ± 3.32	23.1 ± 9.72	18.1 ± 11.2	200 ± 55.3	6.24 ± 5.74	31.5 ± 6.73
Groundwater	683 ± 95.7	24.6 ± 7.99	89.7 ± 30.9	67.8 ± 25.7	614 ± 137	3.31 ± 3.57	88.2 ± 8.35

dissolved ion concentrations at the different study sites were not considered to be caused by differences in the compositions of the base rocks.[9]

The NO_3^- concentrations in the samples collected between 2011 and 2014 were similar to concentrations found between 1996 and 2011 (11.2 ± 3.09 μmol L^{-1} for other regions and 14.6 ± 5.16 μmol L^{-1} in the western region, as shown in Fig. S2†) and in a study performed in 2001 (14.6 ± 5.16 μmol L^{-1} for the western region and 11.2 ± 3.09 μmol L^{-1} for other regions).[6] A survey conducted in December 2023 still showed high values in the western region (17.6 ± 8.00 μmol L^{-1} for the western region and 12.8 ± 11.8 μmol L^{-1} for other regions). We collected samples from rivers in catchment areas >97% covered by forest (Table 1). Agriculture land was only found in some places, with an area of less than 0.2 km^2. Field investigations confirmed that the drainage channels did not flow into the rivers at the study sites. Furthermore, no agricultural land and urban areas were found in the western region where NO_3^- was high. The contribution of anthropogenic NO_3^-, *e.g.*, from agriculture, was therefore considered to be negligible. The main sources of NO_3^- in river water were thought to be atmospheric deposition ($NO_3^-{}_{atm}$) and organic matter decomposed by forest organisms ($NO_3^-{}_{re}$), because sea salt contains little NO_3^-.

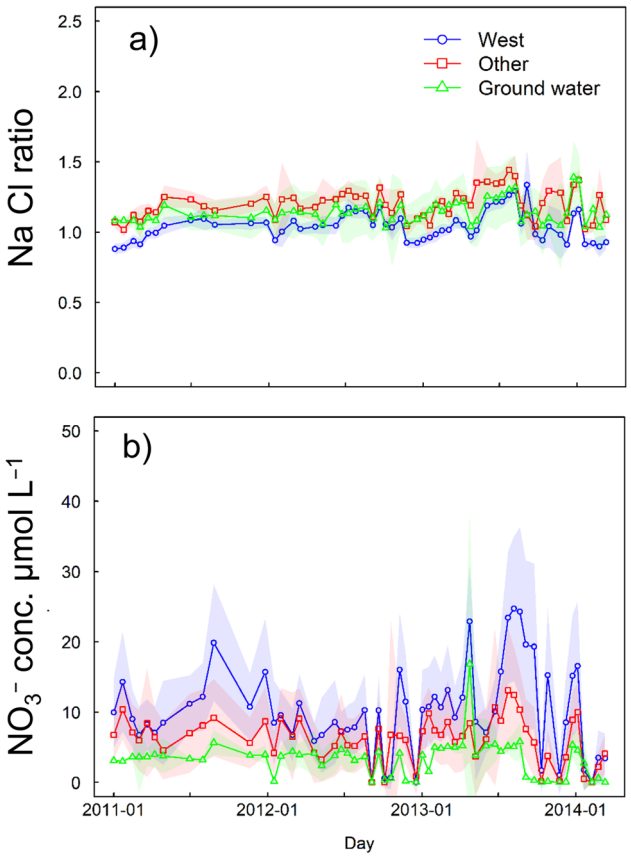

Fig. 3 (a) Na Cl ratios and (b) NO_3^- concentrations in each area determined in the long-term monitoring study. Blue lines indicate rivers in the western region, red lines indicate rivers in the other regions, and green lines indicate groundwater.

The amount of wet nitrogen deposition (NO_3^- and NH_4^+) from the atmosphere observed during the survey period is shown in Fig. S4.† The annual average value from 2011 to 2014 was 9.46 ± 1.76 kg N ha^{-2} per year, and deposition tended to be lower in the summer (0.364 ± 0.276 kg N ha^{-2} $month^{-1}$ from July to September). This value is similar to that of Fukuoka City in Kyushu, Japan (9.7 kg N ha^{-2} per year),[46] which is relatively close to Yakushima Island. High NO_3^- are observed in forest river water around Fukuoka City.[27] Such high NO_3^- in forest river water is commonly observed in suburban forests in the United States,[42,70] Japan,[29,30] and China.[39,71] In forest rivers with a large amount of nitrogen atmospheric deposition, NO_3^- in river water tended to be high (120 μmol L^{-1}),[29] but on Yakushima Island it was very low (14.6 or 11.2 μmol L^{-1}). The annual rainfall in Fukuoka is 1600 mm, while that in Yakuhsima is 4000 mm. This large difference in rainfall had a significant impact on deposition and NO_3^- in river water.

The NO_3^- concentration tended to be higher in the western region than the other regions because of enrichment caused by atmospheric fallout in the western region. Higher non-sea-salt-derived SO_4^{2-} and NO_3^- concentrations originating in continental Asia were found in the western region than the other regions.[3] The topography of the western region causes atmospherically transported substances to accumulate. The terrain in the western region causes fog to form because the mountains are close to the sea and the slopes are covered with forests. Air rich in water vapor rises up the mountain slopes because of valley winds and fog and mizzle forms when the dew point is reached. Pollutants are deposited in relatively large amounts through dry deposition, particularly in winter when fog tends to form.[6] Atmospheric components tend to dissolve more readily in fog and mizzle than rain because fog and mizzle droplets have large surface areas.[72,73] Fog is an important nitrogen deposition pathway in forest ecosystems, particularly in the canopy.[74] Similarly, the NO_3^- concentration tended to be markedly higher in western Yakushima Island, where fog was more likely to occur, than other areas. The Na and Cl ratios for river water from the western region suggested that atmospheric deposition was an important source of various components. The western region is strongly affected by anthropogenic pollutants in winter because of the prevailing westerly winds.[9] It is, therefore, very likely that river water in the western region

contains large amounts of NO_3^- derived from atmospheric nitrogen, particularly in winter. We investigated the source of NO_3^- in the rivers in the forests of Yakushima Island in winter using stable isotope ratios.

3.2 NO_3^- concentrations and stable isotope ratios in major rivers in winter 2018

The NO_3^- concentrations in the river water samples collected in December 2018 are shown in Fig. 4a. The NO_3^- concentrations in river water from the other and western regions were 14.2 and 19.1 μmol L^{-1}, respectively. Similar to the concentrations found between 1996 and 2014 (Fig. S2†), the NO_3^- concentration was higher in the western region than other regions. The NO_3^- concentration in groundwater was 10.3 μmol L^{-1}. NO_3^- concentrations of 11.3 and 15.8 μmol L^{-1} were found in precipitation during the study period (Table 2). The concentrations of other ions followed similar trends from 2011 to 2014 (Fig. S3†).

The $\delta^{15}N$, $\delta^{18}O$, and $\Delta^{17}O$ values for NO_3^- sampled in December 2018 are shown in Fig. 4b–d, respectively. $\Delta^{17}O$ was calculated by eqn (1). The $\delta^{15}N$ values ranged from −1.15‰ to +3.48‰ in other regions, −1.53‰ to +2.27‰ in the western region, and −1.50‰ to +2.70‰ in groundwater (Fig. 4b). The $\delta^{18}O$ values ranged from +0.49‰ to +11.2‰ in other regions, −2.98‰ to +21.2‰ in the western region, and −6.30‰ to +0.23‰ in groundwater (Fig. 4c). These values were within the same ranges as previously found for mountainous areas.[75–77] The $\Delta^{17}O$ values ranged from +0.7‰ to +2.7‰ in other regions, +0.8‰ to +4.9‰ in the western region, and +0.4‰ to +0.8‰ in groundwater (Fig. 4d). Sampling in this study was conducted on clear days. Therefore, it is possible that storm flow, immediately after rain, could produce an outflow of approximately four times as much NO_3^-. Furthermore, it is possible that rainfall could increase the $\Delta^{17}O$ by five times.[78]

We next investigated the sources of NO_3^- in river water in December 2018 using these three stable isotope ratios. The annual mean temperature on Yakushima Island was 20 °C, but the monthly mean temperature for December was 13.7 °C. Microbial activity becomes slower in winter, thus the amount of NO_3^- supplied to river water through microbial metabolism ($NO_3^-{}_{re}$) decreases.[79,80] During periods of winter-type atmospheric pressure patterns, air that has passed over continental Asia reaches Yakushima Island and NO_3^- derived from the atmosphere ($NO_3^-{}_{atm}$) can be a strong source of NO_3^- in river water.

The $\Delta^{17}O$ values in the rivers in December 2018 were +0.5‰ to +4.9‰, which were comparable with the values previously found for natural surface water (−1.4‰ to +6.8‰).[36,42,52,57,78,81] Tsunogai *et al.*[36] studied a mountainous island similar to Yakushima Island, but in a more northern area. NO_3^-, $\delta^{15}N$ and $\Delta^{17}O$ showed similar values to other regions, but $\delta^{18}O$ was higher on Yakushima Island. Molecular oxygen from the surrounding water also affects the $\delta^{18}O$ of oxygen molecules in NO_3^-.[82,83] The amount of precipitation on Yakushima Island is

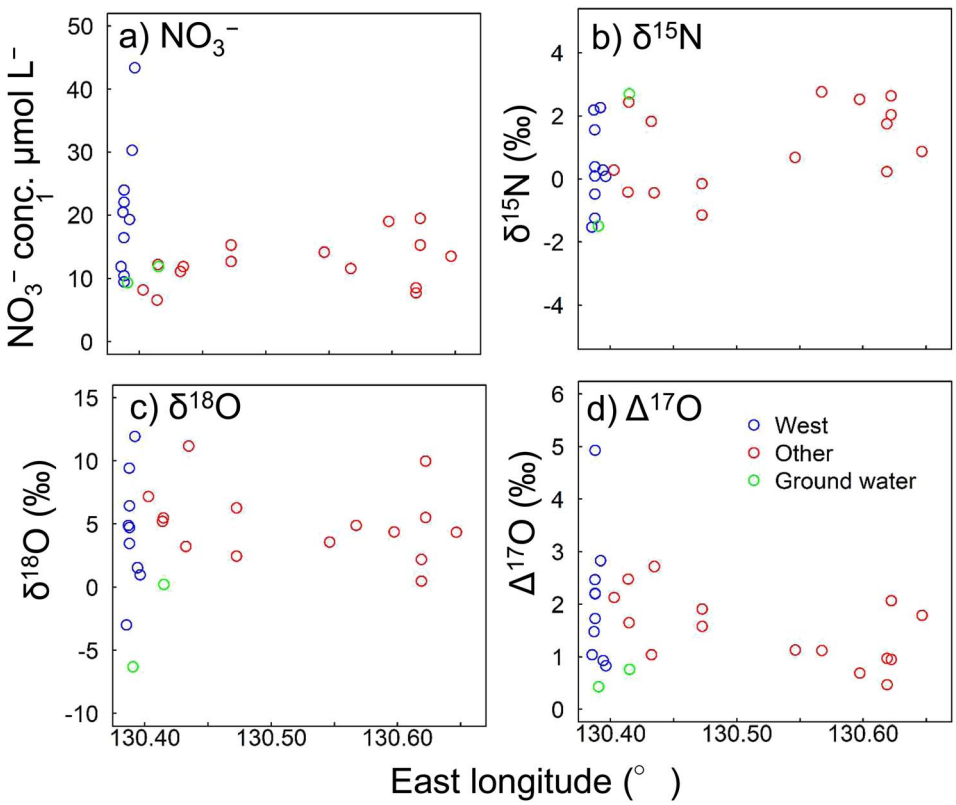

Fig. 4 (a) NO_3^- concentrations, (b) $\delta^{15}N$ values, (c) $\delta^{18}O$ values, and (d) $\Delta^{17}O$ values found in December 2018. $\Delta^{17}O$ was calculated using eqn (1).

about 10 times that of previous survey site, which is likely to reflect precipitation from river water. The $\Delta^{17}O$ in the western region was close to the highest values. Ding *et al.*[46] observed atmospheric deposition of 9.7 kg N ha^{-1} per year, which is one of the highest in forested areas in Japan, and Yakushima Island showed a similar nitrogen deposition amount (9.3–11.2 kg N ha^{-1} per year). However, while the stream water in the previous study[46] contained high NO_3^- (110 μmol L^{-1}), the level in the western region was only about one-third that of the previous study. The contributions of $NO_3^-{}_{re}$ to total NO_3^- were 81.3–98.2% for river water and 97.1–98.4% for groundwater. These results indicated that most of the NO_3^- in river water was supplied through biological nitrification and that very little was supplied from the atmosphere directly. Detailed analysis of the $\Delta^{17}O$ values for the rivers indicated that the atmosphere supplied a larger proportion of nitrate in the western region than in other regions. $NO_3^-{}_{atm}$ generally enters river water when high levels of precipitation fall and when snow melts.[38] Samples were collected during the winter, but no snow fell on Yakushima Island before the sampling period (when the mean temperature was 15.3 °C 60 m above sea level). Less precipitation falls in the western region than in the central part of the island.[84] The high $\Delta^{17}O$ values in the western region could not, therefore, be attributed to high levels of precipitation or melting snow.

The $\Delta^{17}O$ values may have been higher in the western region than the other regions because of differences in water residence times caused by the topographies of the watersheds. There are large differences between watersheds in the western region and other regions. The differences in topography affect the time taken for precipitation to enter the rivers. The longer the water residence time, the more dissolved NO_3^- in river water will be supplied by organisms. The topography of Yakushima Island is diverse and is particularly different in the western region compared with the other regions. The relationships between topographic indices and the NO_3^- and $NO_3^-{}_{atm}$ concentrations in the river watersheds were, therefore, investigated.

3.3 Effects of topography on variations in the nitrate concentration and sources

Topographic analysis for a wide area was performed to determine why the $NO_3^-{}_{atm}$ contribution to the total NO_3^- concentration was higher in the western region than other regions. $NO_3^-{}_{atm}$ was calculated by substituting the value for precipitation in the Northern Hemisphere, +26.6‰,[36,57] into eqn (2). Three topography indicators were compared with the NO_3^- and $NO_3^-{}_{atm}$ concentrations. These were the catchment area, mean catchment slope, and mean catchment TWI. The TWI was calculated using eqn (3). Plots of the NO_3^- and $NO_3^-{}_{atm}$ concentrations against the topography indicators are shown in Fig. 5. The catchment area was negatively correlated with the NO_3^- concentration (Fig. 5a) ($NO_3^-{}_{atm} = -8.99TWI + 21.7$), indicating that the NO_3^- concentration increased as the catchment area decreased. The TWI was negatively correlated with the $NO_3^-{}_{atm}$ concentration ($NO_3^-{}_{atm} = -2.47TWI + 13.3$), indicating that the $NO_3^-{}_{atm}$ concentration increased as the TWI decreased (Fig. 5f). The TWI is a useful indicator of the ease with which water (including surface water and groundwater) collects in a catchment.[61] The TWI of a watershed is, therefore, widely used as an indicator of microbial metabolism (including denitrification, assimilation processes, and nitrification processes that contribute NO_3^- to river water).[62–65] Hayakawa *et al.*[66] found that NO_3^- removal from river water through denitrification occurs in catchments with high TWI values.

The NO_3^- concentration tended to be higher in smaller catchments (Fig. 5a). In general, the larger the watershed area, the more dissolution of rock components and metabolism by organisms occurs. However, on Yakushima Island, NO_3^- concentrations tended to be lower in largely forested areas than elsewhere. River parameters for Yakushima Island reflect precipitation parameters well, and the rivers have short residence times.[85] This suggests that in an area with extremely high rainfall, such as Yakushima Island, the ease with which water runs off because of the topography may strongly affect the sources of NO_3^- in the river water. In a watershed with a relatively large catchment area, the NO_3^- concentration in river water will probably decrease because NO_3^- will be used by trees and other organisms. The sampling sites were in catchments dominated by forests, thus it is likely that differences in runoff processes cause the NO_3^- concentration to increase as the catchment area decreases. However, no clear relationships between the TWI (an indicator of water ponding) and the NO_3^- concentration was found ($R^2 = 0.35$, $p = 0.003$), as shown in Fig. 5d.

The survey was carried out in winter when precipitation on Yakushima Island is low, thus the rivers were at base flow. The direct effects of topography on changes in $NO_3^-{}_{atm}$ concentrations within watersheds through denitrification and biological processes such as nitrification and uptake will be complex.[86] The base rock of Yakushima Island is granite, which has been weathered by long-term acidic deposition,[5] and the high precipitation rate tends to cause a short groundwater residence time. Many rivers in the western region have low TWI values (Table 1). As shown in Fig. 5a, b, d and e, the rivers in the western region have low TWI values because they have small catchment areas and steep terrain. This indicates that rain that falls in the forests will remain for a short period in the soil and bedrock, particularly in the western region. The results suggested that, in the western region, water containing NO_3^- that has not been affected by $NO_3^-{}_{re}$ from forests is discharged into streams. This may explain why atmospheric NO_3^- is affected less by the terrestrial nitrogen cycle in the western region than other regions. The low TWIs may cause both the $NO_3^-{}_{atm}$ and NO_3^- concentrations to be higher in the western region than other regions.

Atmospheric deposition is the main source of nitrogen compounds entering the Yakushima Island ecosystem.[87] Trees on Yakushima Island absorb most of the components supplied by the atmosphere.[88] In this study, we found a strong negative correlation between the catchment area and NO_3^- concentration and a strong relationship between the $NO_3^-{}_{atm}$ concentration and the TWI (Fig. 5f). $NO_3^-{}_{atm}$ deposited in a forest will rapidly become incorporated into the nitrogen cycle within the

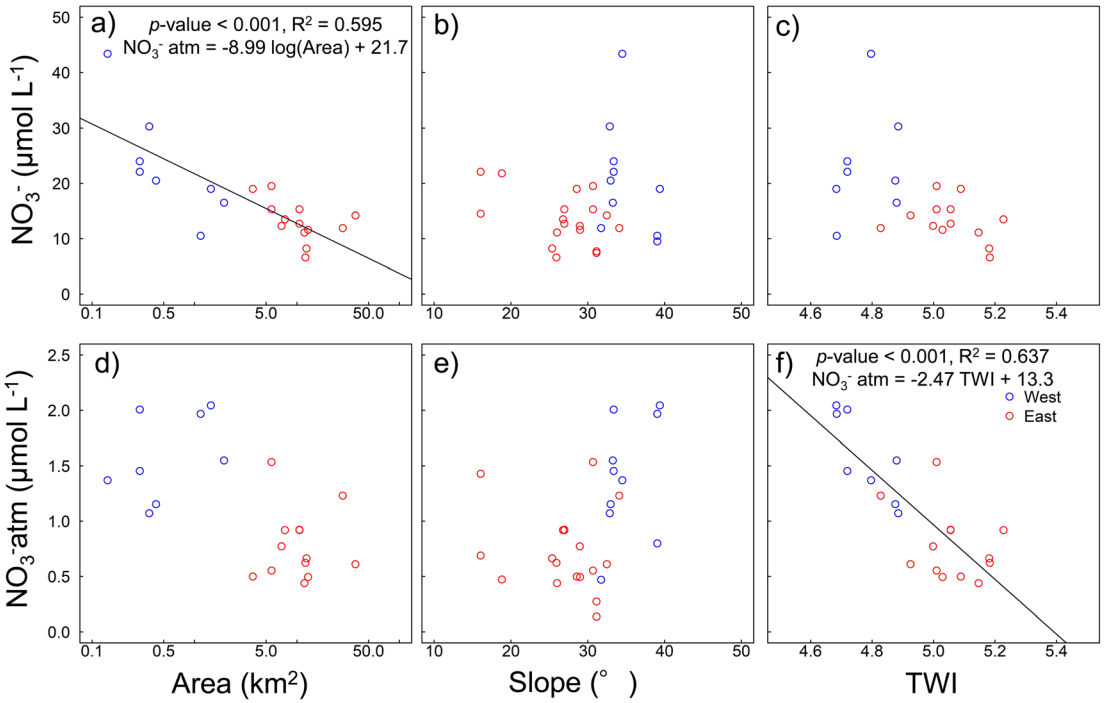

Fig. 5 Relationships between topography parameters (watershed area, watershed mean slope, and topographic wetness index (TWI)) and the (a)–(c) NO_3^- and (d)–(f) $NO_3^-{}_{atm}$ concentrations $NO_3^-{}_{atm}$ was calculated by eqn (2).

forest system.[31] This indicates that atmospheric deposition of $NO_3^-{}_{atm}$ is an important source of nutrients for the forests on Yakushima Island and that the rivers through which $NO_3^-{}_{atm}$ is likely to flow to sea are determined by the water retention capacities of the watersheds. The NO_3^- and $NO_3^-{}_{atm}$ concentrations are higher in the western region than other regions because more atmospheric deposition occurs but also the topography facilitates runoff of $NO_3^-{}_{atm}$. Despite the reduction in atmospheric deposition, NO_3^- in river water remained high in 2023 (Fig. S2†). The results obtained in 2018, therefore, reflect the mechanism of nitrogen cycling in Yakushima's forests.

4 Conclusions

This study has provided insights into the sources of NO_3^- in the rivers on Yakushima Island, revealing that high NO_3^- concentrations are primarily driven by atmospheric deposition. By using stable isotope ratios, we were able to differentiate between $NO_3^-{}_{atm}$ and $NO_3^-{}_{re}$, allowing for a more accurate quantification of $NO_3^-{}_{atm}$ in river water. The rivers on Yakushima Island were categorized into three groups based on the similarity of their dissolved ion compositions: rivers in the western part of the island, rivers in other regions, and groundwater. Notably, NO_3^- concentrations in the western region were 10.5 μmol L^{-1} higher than in other areas, including groundwater, with the majority of these watersheds located within the Natural World Heritage site. Stable isotope analysis confirmed that the western region had higher levels of $NO_3^-{}_{atm}$, suggesting that atmospheric nitrate ions contribute more significantly to river water in this area. Interestingly, the $\Delta^{17}O$ values in the western region mirrored those found in forests with high nitrate runoff, indicating a similar process might be at play. Despite high levels of wet deposition—comparable with those observed in other Asian regions—the overall NO_3^- levels in Yakushima's stream water were relatively low, likely because of the island's significant rainfall. Topographic analysis revealed strong correlations between catchment area, NO_3^- concentration, and TWI, suggesting that smaller watersheds with steep topography are particularly prone to higher $NO_3^-{}_{atm}$ inputs in river water. In nitrogen-limited forest ecosystems, NO_3^- deposited from the atmosphere is typically rapidly assimilated by organisms and converted into $NO_3^-{}_{re}$. However, the unique combination of high precipitation, small watersheds, and steep topography on Yakushima Island appears to limit this biological uptake, allowing a greater proportion of $NO_3^-{}_{atm}$ to enter the rivers directly. Given these findings, it is essential to consider that nitrogen deposition from the atmosphere may vary across different regions of Yakushima. In particular, the western region, where fog is more prevalent, may experience higher levels of nitrogen deposition owing to the concentration of atmospheric constituents in wet deposition from fog. Future studies should aim to clarify the impact of different types of wet and occult deposition on NO_3^- levels in river water and further investigate the relationship between $NO_3^-{}_{atm}$ concentrations and topography in other forested regions with similar conditions.

Data availability

Raw data were generated at Gifu University, Fukuoka Institute of Technology and Setsunan University. Derived data

supporting the findings of this study are available from the corresponding authors K. S.

Author contributions

K. S., O. N., and S. E. conceived the study; K. S., O. N., and S. E. designed the research; K. S., K. T., N. T., O. N., and S. E. led the field work; K. S., K. N., U. T., and F. N. performed laboratory analysis; K. S. performed data analysis and wrote the paper with input from all co-authors.

Conflicts of interest

There are no conflicts to declare.

Acknowledgements

This work was supported by JSPS KAKENHI (grant numbers 26257301, 18K04413 and 23K14057), the Ministry of the Environment Biodiversity Conservation Promotion Support Project, Yakushima Biodiversity Conservation Council, the Institute for Space–Earth Environmental Research (ISEE), Nagoya University, and the Sasakawa Scientific Research (through a grant from the Japan Science Society). The authors are grateful to the students at each university who taught the analytical methods. We thank Gareth Thomas, PhD, and Leonie Seabrook, PhD, from Edanz (**https://jp.edanz.com/ac**) for editing a draft of this manuscript.

References

1 Ministry of the Environment Government of Japan Acid rain monitoring result, **https://www.env.go.jp/air/acidrain/acidrain.html**, accessed July 2024.

2 S. Agata, M. Ishiki, H. Sakihama, A. Tokuyama, H. Satake and J. Zhang, Characteristics of the chemical composition of groundwater on Tanegashima, Yakushima, and Nakanoshima islands, Kagoshima Prefecture, Japan, *Journal of Groundwater Hydrology*, 2012, **54**, 191–206.

3 T. Nakano, M. Okumura, M. Yamanaka and K. Satake, Geochemical Characteristics of Acidic Stream Water on Yakushima Island, a World Natural Heritage Site, *Water, Air, Soil Pollut.*, 2001, **130**, 869–874.

4 K. Fujii, S. Kanetani and K. Tetsuka, Effects of volcanic parent materials on the acid buffering capacity of forest soils on Yakushima Island, Japan, *Soil Sci. Plant Nutr.*, 2020, **66**, 680–692.

5 I. Yukihiro, N. Osamu, A. Suguru, Y. Kuriko and Y. Kazuhisa, Study on low alkalinity measurement method - application to low alkalinity stream on Yakushima, *Journal of Ecotechnology Research*, 2012, **112**, 109–112.

6 O. Nagafuchi, S. Akune, K. Yoshimura, A. Kume, S. Ebise and K. Tetsuka, Effect of Acid Deposition on the Water Quality Formation of Mountainous Streams in the Western Part of Yakushima Island, a World Natural Heritage Site, *J. Jpn. Soc. Water Environ.*, 2003, **26**, 159–166.

7 T. Nakano, Y. Yokoo, M. Okumura, S.-R. Jean and K. Satake, Evaluation of the Impacts of Marine Salts and Asian Dust on the Forested Yakushima Island Ecosystem, a World Natural Heritage Site in Japan, *Water, Air, Soil Pollut.*, 2012, **223**, 5575–5597.

8 T. Doi, O. Nagafuchi, K. Yokota, K. Yoshimura, S. Akune, T. Yamanaka and S. Miyabe, *Determination of sulfur isotope ratio of sulfate in mountainous streams on Yakushima Island after in-situ collection/concentration of sulfate*, 2011, pp. 135–144.

9 O. Nagafuchi, H. Kakimoto, S. Ebise and M. Ukita, Effects of forests on mountain stream water quality, *Jpn. J. Limnol.*, 2002, **63**, 11–19.

10 T. Ohara, Why is the increase of tropospheric ozone concentration in mountain and island regions in Japan?(⟨Feature 2⟩Influence of long-range transport of air pollution on the Japanese ecosystems), *Jpn. J. Ecol.*, 2011, **61**, 77–81.

11 S. Ebise and O. Nagafuchi, Runoff characteristics of water quality and influence of acid rain on mountainous streamwater on Yakushima Island, *Jpn. J. Limnol.*, 2002, **63**, 1–10.

12 J. P. Kaye and S. C. Hart, Competition for nitrogen between plants and soil microorganisms, *Trends Ecol. Evol.*, 1997, **12**, 139–143.

13 J. S. Baron, H. M. Rueth, A. M. Wolfe, K. R. Nydick, E. J. Allstott, J. T. Minear and B. Moraska, Ecosystem Responses to Nitrogen Deposition in the Colorado Front Range, *Ecosystems*, 2000, **3**, 352–368.

14 J. S. Baron, K. R. Nydick, H. M. Rueth, B. M. Lafrançois and A. P. Wolfe, *High Elevation Ecosystem Responses to Atmospheric Deposition of Nitrogen in the Colorado Rocky Mountains*, ed. U. M. Huber, H. K. M. Bugmann and M. A. Reasoner, Springer Netherlands, Dordrecht, 2005, pp. 429–436.

15 J. S. Baron, C. T. Driscoll, J. L. Stoddard and E. E. Richer, Empirical Critical Loads of Atmospheric Nitrogen Deposition for Nutrient Enrichment and Acidification of Sensitive US Lakes, *Bioscience*, 2011, **61**, 602–613.

16 M. W. Williams and K. A. Tonnessen, Critical loads for inorganic nitrogen deposition in the Colorado Front Range, USA, *Ecological Applications*, 2000, **10**, 1648–1665.

17 M. van der Velde, S. R. Green, M. Vanclooster and B. E. Clothier, Sustainable development in small island developing states: agricultural intensification, economic development, and freshwater resources management on the coral atoll of Tongatapu, *Ecological Economics*, 2007, **61**, 456–468.

18 V. Wasiuta, M. J. Lafrenière, A.-L. Norman and M. G. Hastings, Summer deposition of sulfate and reactive nitrogen to two alpine valleys in the Canadian Rocky Mountains, *Atmos. Environ.*, 2015, **101**, 270–285.

19 E. J. Hundey, S. D. Russell, F. J. Longstaffe and K. A. Moser, Agriculture causes nitrate fertilization of remote alpine lakes, *Nat. Commun.*, 2016, **7**, 10571.

20 L. Nanus, M. W. Williams, D. H. Campbell, E. M. Elliott and C. Kendall, Evaluating Regional Patterns in Nitrate Sources

to Watersheds in National Parks of the Rocky Mountains using Nitrate Isotopes, *Environ. Sci. Technol.*, 2008, **42**, 6487–6493.

21 W. D. Bowman, J. R. Gartner, K. Holland and M. Wiedermann, Nitrogen Critical Loads For Alpine Vegetation and Terrestrial Ecosystem Response: Are We There Yet?, *Ecological Applications*, 2006, **16**, 1183–1193.

22 L. Nanus, J. A. McMurray, D. W. Clow, J. E. Saros, T. Blett and J. J. Gurdak, Spatial variation of atmospheric nitrogen deposition and critical loads for aquatic ecosystems in the Greater Yellowstone Area, *Environ. Pollut.*, 2017, **223**, 644–656.

23 J. N. Galloway and E. B. Cowling, Reactive Nitrogen and the World: 200 Years of Change, *Ambio*, 2002, **31**, 64–71.

24 G. F. McIsaac, M. B. David, G. Z. Gertner and D. A. Goolsby, Nitrate flux in the Mississippi River, *Nature*, 2001, **414**, 166–167.

25 H. W. Paerl, Controlling eutrophication along the freshwater-Marine continuum: dual nutrient (N and P) reductions are essential, *Estuaries Coasts*, 2009, **32**, 593–601.

26 J. Kurokawa and T. Ohara, Long-term historical trends in air pollutant emissions in Asia: Regional Emission inventory in ASia (REAS) version 3, *Atmos. Chem. Phys.*, 2020, **20**, 12761–12793.

27 M. Chiwa, N. Onikura, J. Ide and A. Kume, Impact of N-Saturated Upland Forests on Downstream N Pollution in the Tatara River Basin, Japan, *Ecosystems*, 2011, **15**, 230–241.

28 F. Taketani, M. N. Aita, K. Yamaji, T. Sekiya, K. Ikeda, K. Sasaoka, T. Hashioka, M. C. Honda, K. Matsumoto and Y. Kanaya, Seasonal Response of North Western Pacific Marine Ecosystems to Deposition of Atmospheric Inorganic Nitrogen Compounds from East Asia, *Sci. Rep.*, 2018, **8**, 1–9.

29 M. Chiwa, Long-term changes in atmospheric nitrogen deposition and stream water nitrate leaching from forested watersheds in western Japan, *Environ. Pollut.*, 2021, **287**, 117634.

30 H. Sase, M. Takahashi, K. Matsuda, N. Yamashita, U. Tsunogai, F. Nakagawa, M. Morohashi, H. Yotsuyanagi, T. Ohizumi, K. Sato, J. Kurokawa and M. Nakata, Nitrogen saturation of forested catchments in central Japan - progress or recovery?, *Soil Sci. Plant Nutr.*, 2022, **68**, 5–14.

31 R. Sugimoto and T. Tsuboi, Seasonal and annual fluxes of atmospheric nitrogen deposition and riverine nitrogen export in two adjacent contrasting rivers in central Japan facing the Sea of Japan, *Journal of Hydrology: Regional Studies*, 2017, **11**, 117–125.

32 S. Ebise, O. Nagafuchi and H. Kawamura, Relationships between Acidic Wet Depositions and Water Quality in Mountain Streams on Solitary Islands and High Mountains Facing the Sea of Japan and the East China Sea, *Environ. Sci.*, 2019, **32**, 125–140.

33 N. Ohte, I. Tayasu, A. Kohzu, C. Yoshimizu, K. Osaka, A. Makabe, K. Koba, N. Yoshida and T. Nagata, Spatial distribution of nitrate sources of rivers in the Lake Biwa watershed, Japan: controlling factors revealed by nitrogen and oxygen isotope values, *Water Resour. Res.*, 2010, **46**, W07505.

34 C. Kendall, *Isotope Tracers in Catchment Hydrology*, ed. C. Kendall and J. J. McDonnell, Elsevier, Amsterdam, 1998, vol. 16, pp. 519–576.

35 U. Tsunogai, S. Daita, D. D. Komatsu, F. Nakagawa and A. Tanaka, Quantifying nitrate dynamics in an oligotrophic lake using $\Delta^{17}O$, *Biogeosciences*, 2011, **8**, 687–702.

36 U. Tsunogai, D. D. Komatsu, S. Daita, G. A. Kazemi, F. Nakagawa, I. Noguchi and J. Zhang, Tracing the fate of atmospheric nitrate deposited onto a forest ecosystem in Eastern Asia using $\Delta^{17}O$, *Atmos. Chem. Phys.*, 2010, **10**, 1809–1820.

37 F. Nakagawa, U. Tsunogai, Y. Obata, K. Ando, N. Yamashita, T. Saito, S. Uchiyama, M. Morohashi and H. Sase, Export flux of unprocessed atmospheric nitrate from temperate forested catchments: a possible new index for nitrogen saturation, *Biogeosciences*, 2018, **15**, 7025–7042.

38 I. Bourgeois, J. Savarino, N. Caillon, H. Angot, A. Barbero, F. Delbart, D. Voisin and J. C. Clément, Tracing the Fate of Atmospheric Nitrate in a Subalpine Watershed Using $\Delta^{17}O$, *Environ. Sci. Technol.*, 2018, **52**, 5561–5570.

39 S. Huang, F. Wang, E. M. Elliott, F. Zhu, W. Zhu, K. Koba, Z. Yu, E. A. Hobbie, G. Michalski, R. Kang, A. Wang, J. Zhu, S. Fu and Y. Fang, Multiyear Measurements on $\Delta^{17}O$ of Stream Nitrate Indicate High Nitrate Production in a Temperate Forest, *Environ. Sci. Technol.*, 2020, **54**, 4231–4239.

40 J. T. Bostic, D. M. Nelson, R. D. Sabo and K. N. Eshleman, Terrestrial Nitrogen Inputs Affect the Export of Unprocessed Atmospheric Nitrate to Surface Waters: Insights from Triple Oxygen Isotopes of Nitrate, *Ecosystems*, 2022, **25**, 1384–1399.

41 S. Hattori, Y. N. Palma, Y. Itoh, M. Kawasaki, Y. Fujihara, K. Takase and N. Yoshida, Isotopic evidence for seasonality of microbial internal nitrogen cycles in a temperate forested catchment with heavy snowfall, *Sci. Total Environ.*, 2019, **690**, 290–299.

42 L. A. Rose, E. M. Elliott and M. B. Adams, Triple Nitrate Isotopes Indicate Differing Nitrate Source Contributions to Streams across a Nitrogen Saturation Gradient, *Ecosystems*, 2015, **18**, 1209–1223.

43 R. D. Sabo, D. M. Nelson and K. N. Eshleman, Episodic, seasonal, and annual export of atmospheric and microbial nitrate from a temperate forest, *Geophys. Res. Lett.*, 2016, **43**, 683–691.

44 U. Tsunogai, L. Cheng, M. Ito, D. D. Komatsu, F. Nakagawa and H. Shinohara, Remote determinations on fumarole outlet temperatures in an eruptive volcano, *Geophys. Res. Lett.*, 2016, **43**, 11620–11627.

45 U. Tsunogai, D. D. Komatsu, T. Ohyama, A. Suzuki, F. Nakagawa, I. Noguchi, K. Takagi, M. Nomura, K. Fukuzawa and H. Shibata, Quantifying the effects of clear-cutting and strip-cutting on nitrate dynamics in a forested watershed using triple oxygen isotopes as tracers, *Biogeosciences*, 2014, **11**, 5411–5424.

46 W. Ding, U. Tsunogai, F. Nakagawa, T. Sambuichi, M. Chiwa, T. Kasahara and K. Shinozuka, Stable isotopic evidence for the excess leaching of unprocessed atmospheric nitrate from forested catchments under high nitrogen saturation, *Biogeosciences*, 2023, **20**(3), 753–766, DOI: 10.5194/bg-20-753-2023.
47 G. Oota, *Mountains of Yakushima*, Yaedake Press, 1993.
48 Kyushu Regional Forest Office homepage, https://www.rinya.maff.go.jp/kyusyu/yakusima_hozen_c/gaiyou/kisyou/index.html, accessed November 2023.
49 Yakushima World Heritage Conservation Center web site, https://www.env.go.jp/en/park/yakushima/ywhcc/wh/toroku.html, accessed November 2023.
50 UNESCO World heritage list nomination – IUCN summary 662: Yakushima, https://whc.unesco.org/document/153977, accessed November 2023.
51 U. Tsunogai, T. Kido, A. Hirota, S. B. Ohkubo, D. D. Komatsu and F. Nakagawa, Sensitive determinations of stable nitrogen isotopic composition of organic nitrogen through chemical conversion into N_2O, *Rapid Commun. Mass Spectrom.*, 2008, **22**, 345–354.
52 U. Tsunogai, T. Miyauchi, T. Ohyama, D. D. Komatsu, M. Ito and F. Nakagawa, Quantifying nitrate dynamics in a mesotrophic lake using triple oxygen isotopes as tracers, *Limnol. Oceanogr.*, 2018, **63**, S458–S476.
53 U. Konno, U. Tsunogai, D. D. Komatsu, S. Daita, F. Nakagawa, A. Tsuda, T. Matsui, Y. J. Eum and K. Suzuki, Determination of total N_2 fixation rates in the ocean taking into account both the particulate and filtrate fractions, *Biogeosciences*, 2010, **7**, 2369–2377.
54 D. D. Komatsu, T. Ishimura, F. Nakagawa and U. Tsunogai, Determination of the 15N/14N, 17O/16O, and 18O/16O ratios of nitrous oxide by using continuous-flow isotope-ratio mass spectrometry, *Rapid Commun. Mass Spectrom.*, 2008, **22**, 1587–1596.
55 A. Hirota, U. Tsunogai, D. D. Komatsu and F. Nakagawa, Simultaneous determination of $\delta^{15}N$ and $\delta^{18}O$ of N_2O and $\delta^{13}C$ of CH_4 in nanomolar quantities from a single water sample, *Rapid Commun. Mass Spectrom.*, 2010, **24**, 1085–1092.
56 F. Nakagawa, A. Suzuki, S. Daita, T. Ohyama, D. D. Komatsu and U. Tsunogai, Tracing atmospheric nitrate in groundwater using triple oxygen isotopes: evaluation based on bottled drinking water, *Biogeosciences*, 2013, **10**, 3547–3558.
57 U. Tsunogai, T. Miyauchi, T. Ohyama, D. D. Komatsu, F. Nakagawa, Y. Obata, K. Sato and T. Ohizumi, Accurate and precise quantification of atmospheric nitrate in streams draining land of various uses by using triple oxygen isotopes as tracers, *Biogeosciences*, 2016, **13**, 3441–3459.
58 M. F. Miller, Isotopic fractionation and the quantification of ^{17}O anomalies in the oxygen three-isotope system: an appraisal and geochemical significance, *Geochim. Cosmochim. Acta*, 2002, **66**, 1881–1889.
59 K. C. Weathers, S. M. Simkin, G. M. Lovett and S. E. Lindberg, Empirical modeling of atmospheric deposition in mountainous landscapes, *Ecological Applications*, 2006, **16**, 1590–1607.
60 K. C. Weathers, G. M. Lovett, G. E. Likens and R. Lathrop, The effect of landscape features on deposition to hunter mountain, Catskill Mountains, New York, *Ecological Applications*, 2000, **10**, 528–540.
61 K. J. Beven and M. J. Kirkby, A physically based, variable contributing area model of basin hydrology, *Hydrol. Sci. Bull.*, 1979, **24**, 43–69.
62 A. Ogawa, H. Shibata, K. Suzuki, M. J. Mitchell and Y. Ikegami, Relationship of topography to surface water chemistry with particular focus on nitrogen and organic carbon solutes within a forested watershed in Hokkaido, Japan, *Hydrol. Processes*, 2006, **20**, 251–265.
63 K. Shinozuka, M. Chiwa, I. Tayasu, C. Yoshimizu, K. Otsuki and A. Kume, Differences in stream water nitrate concentrations between a nitrogen-saturated upland forest and a downstream mixed land use River Basin, *Hydrology*, 2017, **4**, 43.
64 R. Sugimoto, T. Tsuboi and M. S. Fujita, Comprehensive and quantitative assessment of nitrate dynamics in two contrasting forested basins along the Sea of Japan using dual isotopes of nitrate, *Sci. Total Environ.*, 2019, **687**, 667–678.
65 S. Makino, N. Tokuchi, Y. Komai and T. Kunimatsu, Environmental factors regulating stream nitrate concentrations at baseflow condition in a large region encompassing a climatic gradient, *Hydrol. Processes*, 2021, **35**, e14200.
66 A. Hayakawa, Y. Funaki, T. Sudo, R. Asano, H. Murano, S. Watanabe, T. Ishida, Y. Ishikawa and S. Hidaka, Catchment topography and the distribution of electron donors for denitrification control the nitrate concentration in headwater streams of the Lake Hachiro watershed, *Soil Sci. Plant Nutr.*, 2020, **66**, 906–918.
67 Geospatial Information Authority of Japan, https://fgd.gsi.go.jp/download/menu.php, accessed October 2023.
68 M. W. Raduła, T. H. Szymura and M. Szymura, Topographic wetness index explains soil moisture better than bioindication with Ellenberg's indicator values, *Ecol. Indic.*, 2018, **85**, 172–179.
69 M. Maechler, P. Rousseeuw, A. Struyf, M. Hubert, K. Hornik, M. Studer, P. Roudier, J. González, K. Kozlowski, E. Schubert and K. Murphy, *Package 'cluster.' Finding Groups in Data*, 2022.
70 E. Joshi, M. R. Schwarzbach, B. Briggs, E. R. Coats and M. D. Coleman, Nutrient leaching potential along a time series of forest water reclamation facilities in northern Idaho, *J. Environ. Manage.*, 2024, **366**, 121729.
71 P. Wang, W. Ouyang, Z. Wu, X. Cui, W. Zhu, R. Jin and C. Lin, Diffuse nitrogen pollution in a forest-dominated watershed: source, transport and removal, *J. Hydrol.*, 2020, **585**, 124833.
72 M. Igawa, E. Hoka, T. Hosono, K. Iwase and T. Nagashima, Analysis and Scavenging Effect of Acid Fog, *Nippon Kagaku Kaishi*, 1991, **1991**, 698–704.
73 M. Igawa, Y. Tsutsumi, T. Mori and H. Okochi, Fogwater Chemistry at a Mountainside Forest and the Estimation of

the Air Pollutant Deposition via Fog Droplets Based on the Atmospheric Quality at the Mountain Base, *Environ. Sci. Technol.*, 1998, **32**, 1566–1572.

74 M. Igawa and Y. Wang, Characteristics of Fog and Drizzle in Yokohama and in Mt. Oyama, Japan, *Water, Air, Soil Pollut.*, 2022, **233**, 533.

75 B. Mayer, E. W. Boyer, C. Goodale, N. A. Jaworski, N. Van Breemen, R. W. Howarth, S. Seitzinger, G. Billen, K. Lajtha, K. Nadelhoffer, D. Van Dam, L. J. Hetling, M. Nosal and K. Paustian, Sources of nitrate in rivers draining sixteen watersheds in the northeastern U.S.: isotopic constraints, in *The Nitrogen Cycle at Regional to Global Scales*, 2002, pp. 171–197.

76 D. H. Campbell, C. Kendall, C. C. Y. Chang, S. R. Silva and K. A. Tonnessen, Pathways for nitrate release from an alpine watershed: determination using $\delta^{15}N$ and $\delta^{18}O$, *Water Resour. Res.*, 2002, **38**, 101–109.

77 D. A. Burns and C. Kendall, Analysis of $\delta^{15}N$ and $\delta^{18}O$ to differentiate NO_3^- sources in runoff at two watersheds in the Catskill Mountains of New York, *Water Resour. Res.*, 2002, **38**, 91–912.

78 G. Michalski, T. Meixner, M. Fenn, L. Hernandez, A. Sirulnik, E. Allen and M. Thiemens, Tracing Atmospheric Nitrate Deposition in a Complex Semiarid Ecosystem Using $\Delta^{17}O$, *Environ. Sci. Technol.*, 2004, **38**, 2175–2181.

79 L. K. Lautz and R. M. Fanelli, Seasonal biogeochemical hotspots in the streambed around restoration structures, *Biogeochemistry*, 2008, **91**, 85–104.

80 S. A. Comer-Warner, D. C. Gooddy, S. Ullah, L. Glover, N. Kettridge, S. K. Wexler, J. Kaiser and S. Krause, Seasonal variability of sediment controls of nitrogen cycling in an agricultural stream, *Biogeochemistry*, 2020, **148**, 31–48.

81 T. Liu, F. Wang, G. Michalski, X. Xia and S. Liu, Using 15N, 17O, and 18O to determine nitrate sources in the Yellow River, China, *Environ. Sci. Technol.*, 2013, **47**, 13412–13421.

82 A. Amberger and H.-L. Schmidt, Natürliche Isotopengehalte von Nitrat als Indikatoren für dessen Herkunft, *Geochim. Cosmochim. Acta*, 1987, **51**(10), 2699–2705, DOI: **10.1016/0016-7037(87)90150-5**.

83 R. F. Spalding, A. J. Hirsh, M. E. Exner, N. A. Little and K. L. Kloppenborg, Applicability of the dual isotopes $\delta^{15}N$ and $\delta^{18}O$ to identify nitrate in groundwater beneath irrigated cropland, *J. Contam. Hydrol.*, 2019, **220**, 128–135, DOI: **10.1016/j.jconhyd.2018.12.004**.

84 H. Takaharra and J. Matsumoto, Climatological Study of Precipitation Distribution in Yakushima Island, Southern Japan, *J. Geogr.*, 2002, **111**, 726–746.

85 M. Yamanaka, M. Okumura and T. Nakano, Isotopic altitude effect and discharge characteristics of river water in Yakushima Island, southwestern Japan, *Journal of Japanese Association of Hydrological Sciences*, 2007, **37**, 41–54.

86 E. M. Lacroix, M. Aeppli, K. Boye, E. Brodie, S. Fendorf, M. Keiluweit, H. R. Naughton, V. Noël and D. Sihi, Consider the Anoxic Microsite: Acknowledging and Appreciating Spatiotemporal Redox Heterogeneity in Soils and Sediments, *ACS Earth Space Chem.*, 2023, **7**, 1592–1609.

87 K. Satake, T. Inoue, K. Kasasaku, O. Nagafuchi and T. Nakano, Monitoring of nitrogen compounds on Yakushima Island, a world natural heritage site, *Environ. Pollut.*, 1998, **102**, 107–113.

88 T. Nakano, S.-R. Jeon, J. Shindo, T. Fumoto, N. Okada and J. Shimada, Sr Isotopic Signature in Plant-Derived Ca in Rain, *Water, Air, Soil Pollut.*, 2001, **130**, 769–774.